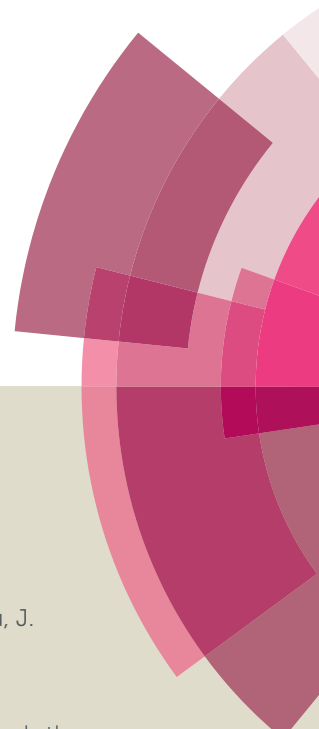


Journal of Materials Chemistry B

Accepted Manuscript



This article can be cited before page numbers have been issued, to do this please use: M. Zhao, Y. Zhu, J. Su, Q. Geng, X. Tian, J. Zhang, H. Zhou, S. Zhang, J. Wu and Y. Tian, *J. Mater. Chem. B*, 2016, DOI: 10.1039/C6TB01240J.



This is an *Accepted Manuscript*, which has been through the Royal Society of Chemistry peer review process and has been accepted for publication.

Accepted Manuscripts are published online shortly after acceptance, before technical editing, formatting and proof reading. Using this free service, authors can make their results available to the community, in citable form, before we publish the edited article. We will replace this *Accepted Manuscript* with the edited and formatted *Advance Article* as soon as it is available.

You can find more information about *Accepted Manuscripts* in the [Information for Authors](#).

Please note that technical editing may introduce minor changes to the text and/or graphics, which may alter content. The journal's standard [Terms & Conditions](#) and the [Ethical guidelines](#) still apply. In no event shall the Royal Society of Chemistry be held responsible for any errors or omissions in this *Accepted Manuscript* or any consequences arising from the use of any information it contains.



Journal Name

ARTICLE

A water-soluble two-photon fluorescence chemosensor for ratiometric imaging mitochondrial viscosity in living cells

Meng Zhao,^a Yingzhong Zhu,^a Jian Su,^a Qian Geng,^b Xiaohu Tian,^{*b} Jun Zhang,^c Hongping Zhou,^a Shengyi Zhang,^a Jieying Wu,^a Yupeng Tian^{*a}

Received 00th January 20xx,
Accepted 00th January 20xx

DOI: 10.1039/x0xx00000x

www.rsc.org/

Convenient and rational design water-soluble two-photon excited fluorescence (TPEF) sensor for monitoring viscosity with specific targeting at subcellular level remain a challenge. Herein, we reported a novel water-soluble ratiometric TPEF chemosensor **EIN** that is specifically responsive and singularly sensitive to mitochondria viscosity in living cells. Because its fluorescence emission bands at two different wavelengths show obvious enhancement with the increased solvent viscosity, we found that fluorescence intensity ratio (I_{569} / I_{384}) versus the logarithm of the viscosity ($\log \eta$) enable to monitor and quantify the abnormal changes of mitochondria viscosity. More importantly, **EIN** was successfully utilized to distinguish normal and nystatin treated HepG2 cells viscosity difference of mitochondria. In a word, the merits of NIR property, high selectivity and signal ratio provide more convenience for studying biological processes and mitochondria viscosity related diseases.

Introduction

Intracellular viscosity is a significant factor governing the mass or signal transportation, biomacromolecules interactions and reactive metabolites diffusion.^{1,2} Abnormal *in vivo* viscosity reflect diseases and malfunctions, such as Alzheimer disease, diabetes, atherosclerosis and cell malignancy.³⁻⁵ In addition, unusual viscosity variation in mitochondrial matrix may induce changes in mitochondrial network organization, and further influence metabolite diffusion.⁶ Therefore, rational designing targeted molecules capable of quantifying the mitochondrial viscosity in living cells are of great significance.

It is known that molecular rotors possess the rotatable conjugated moiety, that is, a certain part of a whole molecular can rotate to another part. On the one hand, the intramolecular rotation relaxes the excitation energy resulting in significant decreasing or quenching of fluorescence in low-viscosity environments. On the other hand, intramolecular rotation is inhibited in viscous environments, which can reduce the probability of nonradiating pathways and further restore fluorescence.^{7,8} Hence, molecular rotors with appropriate biocompatibility are highly suitable as viscosity-sensitive fluorescent chemosensors in living cells and tissues.

In the past decades, molecular rotors with dual emission as the

micro-viscosity-targeted TPEF sensors have been introduced.^{9,10} Such ratiometric detection allows signal rationing and has been widely applied in microviscosity imaging and quantification. However, in view of the fact that many viscosity-related diseases and malfunctions are organelle phenotypic, how to design organelle-specific chemosensor still remains a challenge for biological applications. Since double-layer mitochondria offer high viscosity micro-environments, viscosity sensors capable of exhibiting strong fluorescence emission once combined to the mitochondria, while viscosity sensors exhibit weak or quenching background emission in the uncombined state.¹¹ Considering above, a novel chemosensor **EIN** was designed and synthesized by introducing flexible diethyl 2,2'-(phenylazanediy)diacetate moiety and cationic 1,2,3,3-tetramethyl-3H-indol-1-ium moiety. Compared with reported viscosity sensors,¹²⁻¹⁶ ratiometric TPEF chemosensor **EIN** has great water solubility, low cytotoxicity, reasonable photostability, large Stokes shift as well as longer excitation wavelengths of two-fluorescence microscopy (TPM). Importantly, by means of the fluorescence intensity ratio of 569 and 384 nm, the precise mitochondria viscosity in normal and nystatin treated HepG2 cells was also measured.¹⁷⁻¹⁹

Results and discussion

Design and synthesis of EIN

The organic molecules based on the push-pull π -conjugated system might possess the main and most promising foundation for two-photon materials,^{20,21} especially in the field of chemosensor applications.²²⁻²⁵ Diethyl 2,2'-

^a Department of Chemistry, Key Laboratory of Functional Inorganic Material Chemistry of Anhui Province, Anhui University, Hefei 230039, P. R. China.

^b School of Life Science, Anhui University, Hefei 230039, P. R. China

^c Key Laboratory of Functional Molecule Design and Interface Process, Anhui Jianzhu University, Hefei 230601, P. R. China

*Electronic Supplementary Information (ESI) available: The crystal structural and selected bond lengths and angles. PH effect, cytotoxicity and photostability.

ARTICLE

Journal Name

(phenylazenediyl)diacetate moiety is not only an electron-donating group, but also possess good biocompatibility as well, which suggested that it is highly prospective for constructing biocompatible TPEF sensor for bioimaging in living cells and tissues. Cyanine dye, 1,2,3,3-tetramethyl-3H-indol-1-ium, is a cationic fluorophore with high fluorescence quantum yields, NIR property and great water stability, and it is well established that cationic dyes can be easily taken up and accumulate in the mitochondria of living cells.^{26,27} To design water-soluble ratiometric TPEF chemosensor with mitochondrial specificity, diethyl 2,2'-(phenylazenediyl)diacetate was connected with 1,2,3,3-tetramethyl-3H-indol-1-ium to produce a novel cationic chemosensor **EIN** by using extended π -conjugation double bond, as shown in **Scheme 1**.

Spectral properties

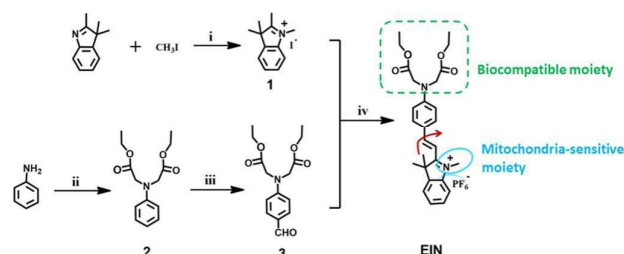
The linear absorption and emission spectra of **EIN** in H₂O buffered with HEPES are shown in **Fig. S2**. It can be seen that **EIN** exhibits two absorption peaks ($\lambda_{\text{abs}} = 320 \text{ nm}$ and 483 nm) and two emission peaks ($\lambda_{\text{em}} = 378 \text{ nm}$ and 562 nm) in pure HEPES buffer. Furthermore, water and glycerol solubility experiments were shown in **Fig. S3**, which suggested that **EIN** possesses good water solubility ($50 \mu\text{M}$) and glycerol solubility ($20 \mu\text{M}$).

One-photon fluorescence response to solvent viscosity

As shown in **Fig. S4**, generally solvents with different polarity influence the absorption and emission maxima to some extent. **EIN** gives very small responses upon polarity, and such limited polarity influence is vital to the molecular rotor to sense environmental viscosity.²⁸⁻³¹

To investigate the relationship between the viscosity and the fluorescent intensity, fluorescence emission spectra of **EIN** was measured upon 320 nm at room temperature as shown in **Fig. 1a**. It is obvious that **EIN** showed two emission bands at 384 nm and 569 nm, where both emission intensities were found to be enhanced by increasing proportions of glycerol in the mixture solvent. The fluorescence intensity of **EIN** at 569 nm increased 29-fold while the blue emission at 384 nm gave weaker responses with the 11-fold fluorescence enhancement. As a result, we found a better linear relationship ($R^2 = 0.994$, the slope $x = 0.464$) between fluorescence intensity ratio (I_{569} / I_{384}) and the logarithm of the viscosity ($\log \eta$).^{32,10} The results exhibited that **EIN** can be employed to ratiometrically detect viscosity in various environments including biological systems (**Fig. 1b** and **Fig. S5**).

In addition, we investigated the red emission spectra ($\lambda_{\text{em}} =$



Scheme 1. Schematic representation of the synthesis procedures of **EIN**.

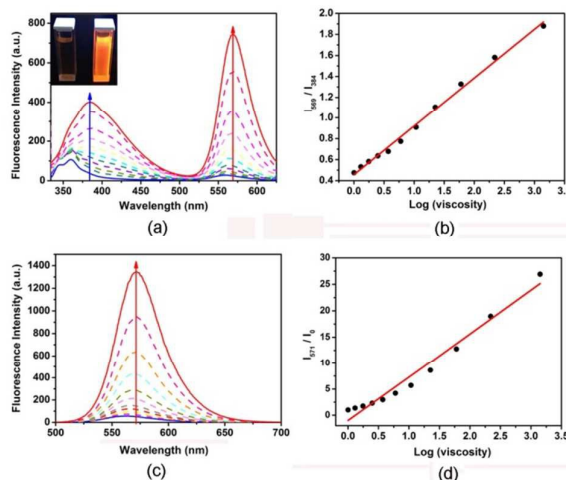


Fig. 1 (a) Changes of fluorescence spectra with the variation of solution viscosity in water-glycerol system (excited at 320 nm). (b) Relationship of fluorescence intensity ratio (I_{569} / I_{384}) with the logarithm of the viscosity ($\log \eta$). (c) Changes of fluorescence spectra with the variation of solution viscosity in water-glycerol system (excited at 490 nm). (d) Relationship of fluorescence intensity ratio (I_{571} / I_{569}) with the logarithm of the viscosity ($\log \eta$). Inset in (a), fluorescence changes of **EIN** in 0.01% or 99.9% glycerol system under UV light (365 nm excitation).

571 nm) of **EIN** with increasing proportions of glycerol in the mixture solvent. The emission of **EIN** was greatly enhanced (24-fold) with the increased solvent viscosity when excited at 490 nm (**Fig. 1c**). And the fluorescence intensity ratio (I / I_0) at 571 nm showed a reasonable linear relationship with logarithm of the viscosity ($\log \eta$) of the solution ($R^2 = 0.970$, the slope $x = 8.299$), which was identical to that measured for the dual emission (**Fig. 1d**).

The study of quantum yield (QY) and fluorescence lifetime of **EIN** were also carried out as shown in **Fig. 2**. Quantum yields were very low, approximately 0.01-0.05, in low-viscosity solvents such as water, methyl alcohol and dimethyl sulfoxide, and was not apparently affected by solvent polarity. However, in water and glycerol mixed solvents (viscosity range from 1.005 cP to 1385 cP), the quantum yields of **EIN** obviously increased with increasing glycerol volume fraction. In 99.9% glycerol, **EIN** exhibited the strongest and naked eye visible red emission with the highest quantum yield 0.33. Namely, **EIN** can exhibit strong fluorescence intensity only in viscous medium restricting intramolecular free rotation and reducing the probability of nonradiating pathways, and other factors such

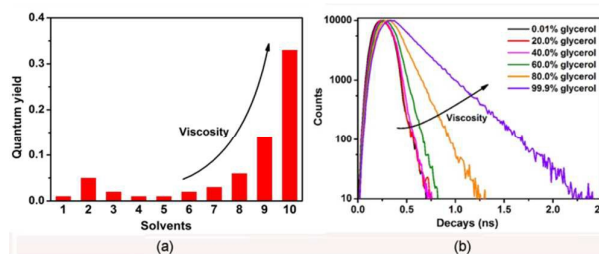


Fig. 2 (a) The fluorescence quantum yields of **EIN** (excited at 490 nm) in different solvents: (1) dichloromethane, (2) dimethyl sulphoxide, (3) ethanol, (4) methanol, (5) water, (6) water/glycerol (8:2, v/v), (7) water/glycerol (6:4, v/v), (8) water/glycerol (4:6, v/v), (9) water/glycerol (2:8, v/v), (10) glycerol (99.9%). (b) Changes of fluorescence decay of **EIN** ($10 \mu\text{M}$) with the variation of solution viscosity, excited at 490 nm.

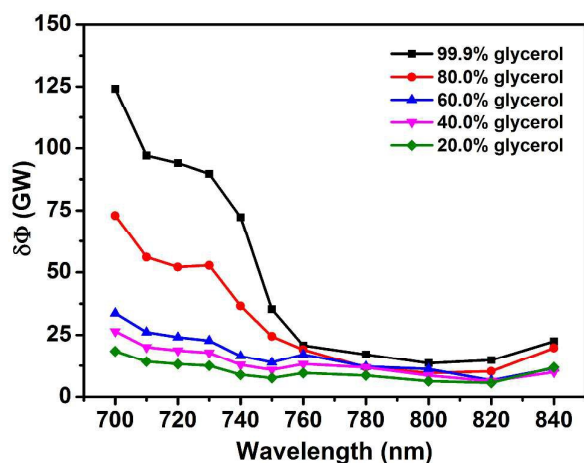


Fig. 3 Two-photon (TP) action cross-section spectra of EIN with the variation of solution viscosity in the wavelength region 700-840 nm.

as pH did not affect bond rotation and alter its fluorescence intensity (Fig. S6).

Two-photon absorption response to solvent viscosity

Since the push-pull π -conjugated system has been reported to possess two-photon properties, the two-photon cross sections of EIN were recorded using two photon excited fluorescence measurements (Fig. 3). The two-photon process was also confirmed by a power dependence experiment (Fig. S7). In the range of 700-840 nm, two-photon absorption spectra of EIN enhanced remarkably (6.9-fold at 700nm) with increasing proportions of glycerol in the mixture solvent. And the two-photon action cross-section ($\Phi\delta$) at 700 nm increased from 18.5 (20 % glycerol, 1.76 cP) to 124.1 GM (99.9 % glycerol, 1385 cP) ($1 \text{ GM} = 10^{-50} \text{ cm}^4 \text{ s photon}^{-1}$). Such remarkable enhancement of two-photon action cross-sections ($\Phi\delta$) is crucial to permit a molecular rotor to reflect environmental viscosity in biological system.

In addition, interference experiments exhibited the fluorescence intensity of EIN rarely responded in the presence of DNA, RNA, BSA and various aminophenol within one hour (Fig. S8).

Cell cytotoxicity (MTT)

The study of the effect of EIN on viability of HepG2 cells was carried out using the methylthiazolyldiphenyl-tetrazolium bromide (MTT) assay as shown in Fig. S9. With the concentration ranging from 10 μM to 50 μM , EIN has little cytotoxicity for 24 hours incubation. Subsequently, photon resistance abilities were evaluated via standard photon-bleaching experiments, indicating that EIN exhibited reasonable photo-stability and showed no significant fluorescence signals decrease under continuous irradiation for 518 s (Fig. S10). Above results promised further two-photon biological imaging in living cells.

Cell localization of EIN

To investigate intracellular distribution of EIN, cell imaging was first performed with HepG2 cells under confocal fluorescence microscopy. As illustrated in Fig. 4 and Fig. S11, micrographs demonstrated EIN (10 μM , 30 min) stained tubular-like structure with superb signal-to-noise ratio. Furthermore to

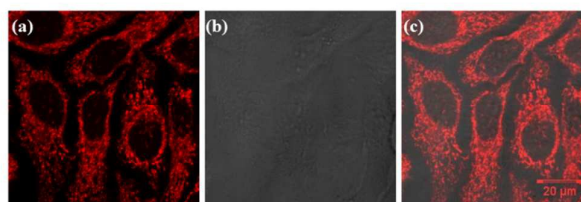


Fig. 4 Confocal laser fluorescence microscopic images of HepG2 cells treated with 10 μM EIN. (a) Fluorescent image of EIN, collected at 520-580 nm and excited at 840 nm; (b) bright fields of HepG2 cells; (c) Merged image of (a) and (b).

evaluated the precise subcellular localization of EIN, colocalization experiments using commercial dyes were evaluated (Mito Tracker Red: panels (a) – (c), Lyso-Tracker blue: panels (d) – (f)) as showed in Fig. 5. Apparently, EIN exhibited superior mitochondria-targeting ability than lysosomes with colocalization coefficient of 0.90 and 0.05, respectively (Fig. 6). The above experimental results implied that EIN is indeed a mitochondria-targeted two-photon fluorescence sensor.

In addition, we inspected whether mitochondrial membrane potential could influence the fluorescence signals of EIN since it accumulates in mitochondria (Fig. 7). Then HepG2 cells treated with a membrane-potential uncoupler CCCP that disrupt mitochondrial membrane potential were simultaneously incubated Mito Tracker Red or EIN.³³⁻³⁵ Staining with Mito Tracker Red whose uptake is dependent of mitochondria membrane potential was inconsistent in the absence or presence of CCCP. Similarly, fluorescence brightness of EIN changed distinctly upon treatment with CCCP. The above results implied that EIN locate in mitochondria in living are membrane potential dependent.

Ratiometric two-photon fluorescence imaging

Since one of major advantages of mitochondria-targeted EIN is that it possesses dual absorption and emission, that is independent of the dye concentration or intracellular distribution, and avoid most of the interferences from

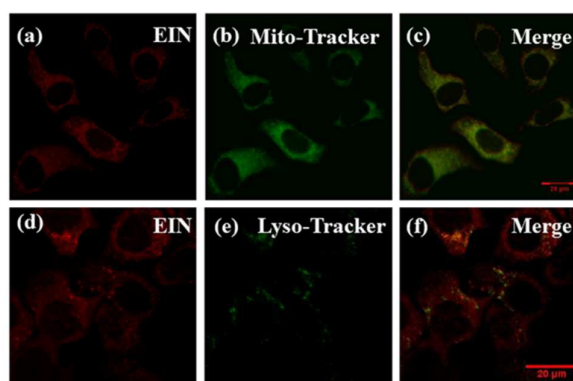


Fig. 5 Confocal laser fluorescence microscopic images of HepG2 cells treated with 10 μM EIN and Mito-tracker Red (1.0 μM) or Lyso-Tracker Blue (1.0 μM). (a) and (d) Fluorescence imaging of EIN in HepG2 cells, collected at 520-580 nm and excited at 840 nm; (b) Fluorescent image of Mito-Tracker Red (1.0 μM), collected by a 585-625 nm band path filter with excitation at 579 nm; (c) Merged image of (a) and (b); (e) Fluorescent image of Lyso-Tracker Blue (1.0 μM), collected by a filter of 410-450 nm upon excitation at 408 nm; (f) Merged image of (d) and (e).

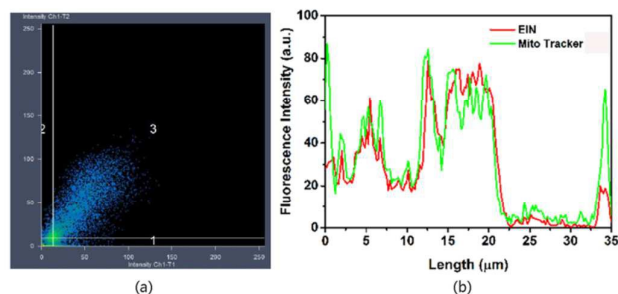


Fig. 6 (a) Correlation plot of Mito-Tracker Red and EIN intensities. (b) Intensity profile of ROIs across HepG2 cells.

microenvironments.³⁶⁻³⁸ Therefore we consider **EIN** is highly suitable to quantify mitochondrial viscosity and monitor its abnormal change in living cells. As shown in **Fig. 8**, the fluorescence images were obtained by collecting the blue emission region (375 – 450 nm) and the red emission region (520 – 580 nm) when excited at 840 nm. The ratio image (panels (d) and (h)) based on blue emission and red emission clearly displayed the distribution of viscosity in the cells. And the average fluorescence intensity ratio in HepG2 cells is 1.27 ± 0.05 (panels (d)), which is equivalent to 56.7 cP according to linear relationship between fluorescence intensity ratio and the logarithm of the viscosity. Moreover, upon treatment with nystatin (panels (e) – (h)), which can induce mitochondrial malfunction caused by structure changes or swelling of mitochondria,^{39,40} the average viscosity of mitochondria in HepG2 cells increased to 199.3 cP (average fluorescence intensity ratio is 1.52 ± 0.05 , panels (h)). Obviously, the green regions in panels (d) and (h) represent higher viscosity than blue regions. Above experimental results agrees with previous reports and indicates that nystatin can induce abnormal increasing of mitochondria viscosity. Accordingly, **EIN** as a mitochondrial viscosity chemosensor can monitor and quantify abnormal metabolic changes in mitochondria with high

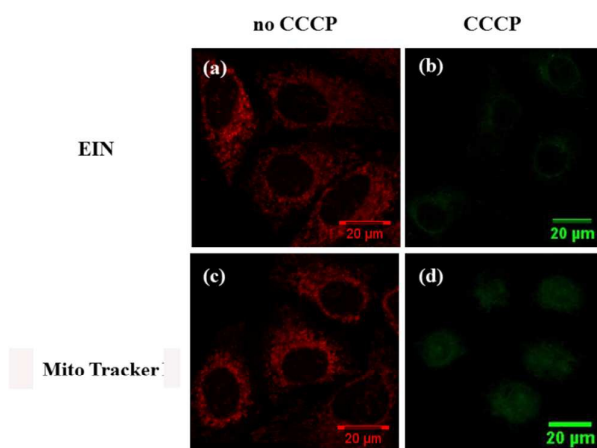


Fig. 7 Confocal laser fluorescence microscopic images of HepG2 cells treated with 10 μM **EIN** or 1.0 μM Mito-tracker Red, then the cells were incubated in the absence or presence of 10 μM CCCP for 30 min. (a) and (b) Fluorescent image of **EIN**, collected by a 520-580 nm band path filter with excitation at 840 nm; (c) and (d) Fluorescent image of Mito-tracker Red, collected by a 585-625 nm band path filter with excitation at 579 nm.

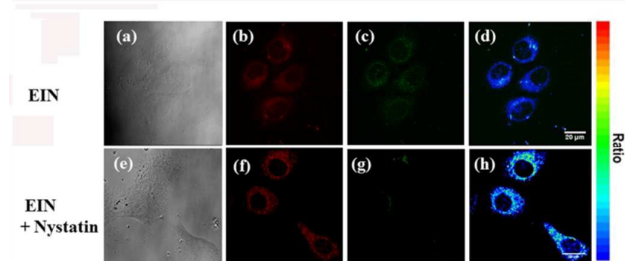


Fig. 8 Confocal laser fluorescence microscopic images of 10 μM **EIN** before and after treatment of HepG2 cells by 10 μM nystatin for 30 minutes, respectively; (a) and (e) Bright fields of HepG2 cells; (b) and (f) Red channels fluorescence images detected at 520-580 nm upon excited at 840 nm; (c) and (g) Green channels fluorescence images detected at 375-450 nm upon excited at 840 nm; (d) and (h) Ratiometric image of **EIN** obtained by the ImageJ software.

accuracy and reliability.

Conclusion

To summarize, a viscosity-sensitive water-soluble TPEF chemosensor with a flexible diethyl 2,2'-(phenylazanediy)diacetate moiety and cationic 1,2,3,3-tetramethyl-3H-indol-1-ium moiety have been developed. As a water-soluble cationic sensor, it has dual absorption and emission, as well as large two-photon action cross-sections ($\Phi\delta$). Other factor such as the polarity of solvents has limited influence on sensor **EIN**. Also, it exhibits reasonable photostability and low cytotoxicity and can effectively stain mitochondria by mitochondrial membrane potential. Fluorescence intensity ratio (I_{569} / I_{384}) of **EIN** is in better linear relationship with the logarithm of the viscosity ($\log \eta$) ($R^2 = 0.994$, the slope $x = 0.464$). Thus the **EIN** is able to quantitatively track and image the intracellular mitochondria viscosity by fluorescence ratiometry with excellent self-calibrating ability. Furthermore, **EIN** was successfully applied for monitoring the viscosity distinction in normal and nystatin treated HepG2 cells. It is anticipated that **EIN** provide a promising strategy for the pathology investigation and diagnoses of mitochondria viscosity related diseases.

Experimental

Materials and physical measurements

All chemicals and solvents used in the synthesis were of reagent grade and used without further purification while handling them. The $^1\text{H-NMR}$ spectra were recorded at 25 $^\circ\text{C}$ on a Bruker Advance 400 spectrometer, and the chemical shifts are reported as parts per million from TMS (δ). The $^{13}\text{C-NMR}$ spectra were recorded on 150 MHz spectrometers. Chemical shifts were reported in parts per million relative to tetramethylsilane ($\delta = 0$). Mass spectra were determined with a Micro-mass GCT-MS (EI source). Elemental analyses were measured on a Perkin Elmer 240C elemental analyzer. FT-IR spectra (KBr pellets) were recorded with a NEXUS-870 (Nicolet) spectrometer in the 4000-400 cm^{-1} region. The linear absorption spectra were measured on a SPECORD S600 spectrophotometer. The single-photon emission fluorescence

(SPEF) spectra measurements were performed using a Hitachi F-7000 fluorescence spectrophotometer. The two-photon emission fluorescence (TPEF) spectra were measured at femtosecond laser pulse and Ti: sapphire system (680-1080 nm, 80 MHz, 140 fs) as the light source. The viscosities of the solvents were determined using capillary Ubbelohde dilution type viscometers, and higher viscosities of the aqueous solution of glycerol were taken from published tables.¹⁹ The fluorescent quantum yields were measured with integrating sphere.

HepG2 cells were luminescently imaged on a Zeiss LSM 710 META upright confocal laser scanning microscope. Image data acquisition and processing was performed using Zeiss LSM Image Browser, Zeiss LSM Image Expert and Image J.

Synthesis of compound 1

2,3,3-Trimethylindolenine (1.59 g, 10.0 mmol) was dissolved in iodomethane (3.98 g, 28.0 mmol) and with constant stirring, the solution was refluxed for 24 hours. The precipitate produced was filtered under suction, washed with n-hexane and dried in vacuo to yield the product as a pink solid (1.7 g, yield 56 %).⁴¹

Synthesis of compound 2

Aminobenzene (1.86 g, 20.0 mmol) was dissolved in acetonitrile (25.0 mL) under nitrogen and with constant stirring, followed by the addition of potassium iodide (7.30 g, 44.0 mmol), potassium carbonate (6.08 g, 44.0 mmol) and ethyl bromoacetate (7.35 g, 44.0 mmol). With constant stirring, the solution was refluxed for 12 hours to produce a brown solution. Then the mixture was cooled, the filtrate was concentrated to yield brown oil as crude product (4.4 g, 86 %).⁴²

Synthesis of compound 3

Phosphorus oxychloride (6.52 g, 42.5 mmol) was added dropwise to a cooled solution of dimethylformamide (3.11 g, 42.5 mmol) over a period of 1 hour keeping the temperature below 5 °C during the addition. After the frozen salt appeared, compound 2 was added and with constant stirring at room temperature for 12 hours. The mixture was poured into a large amount of ice water and adjusted to pH = 8 using 1 mol/L sodium hydroxide. The precipitate produced was filtered under suction, washed with water and dried in vacuo to yield the product as a yellow solid. The solid was purified by silica gel chromatography column using petroleum/ethyl acetate (5/1, v/v) as the eluent, and compound 3 was obtained as yellow solid as crude product (0.87 g, 36%).⁴²

Synthesis of EIN

Compound 3 (0.98 g, 3.40 mmol) was dissolved in acetonitrile (20.0 mL), followed by the addition of compound 1 (1.00 g, 3.20 mmol). With constant stirring, five drops of piperidine were added to the mixture, and the solution was refluxed for 12 hours to produce a red solution. After cooling, AgPF₆ (0.81 g, 3.20 mmol) was added dropwise into the solution with constant stirring at 60 °C for 1 hour. The solution was concentrated under reduced pressure to yield red oil, which was purified by column chromatography using dichloromethane/methanol (10:1, v/v) as the eluent, and EIN was collected as red solid (1.20 g, 61%).

Elemental analysis for EIN, C₂₇H₃₃F₆N₂O₂P, Calcd (%): C, 57.65; H, 5.91; N, 4.98. Found: C, 55.30; H, 5.57; N, 4.75. ¹H-NMR (d₆-DMSO, 400 MHz, ppm) δ = 8.32 (d, J = 15.9 Hz, 1H), 8.07 (d, J =

8.7 Hz, 2H), 7.78 (dd, J = 15.8, 7.7 Hz, 2H), 7.55 (dd, J = 14.0, 7.4 Hz, 2H), 7.37 (d, J = 16.0 Hz, 1H), 6.80 (d, J = 8.8 Hz, 2H), 4.43 (s, 4H), 4.15 (q, J = 7.0 Hz, 4H), 4.02 (s, 3H), 1.75 (s, 6H), 1.22 (t, J = 7.1 Hz, 6H). ¹³C-NMR (d₆-DMSO, 101 MHz, ppm) δ = 180.5, 169.4, 153.8, 152.8, 142.9, 141.9, 133.3, 128.7, 128.1, 123.8, 122.6, 114.1, 112.5, 107.2, 60.8, 52.5, 51.3, 33.4. FT-IR (KBr, ν, cm⁻¹): 2985(vw), 2363(vw), 2345(vw), 1744(m), 1577(s), 1529(vs), 1479(m), 1420(w), 1396(m), 1374(w), 1332(w), 1301(m), 1189(vs), 1173(s), 1164(s), 1117(m), 1021(w), 972(w), 932(vw), 840(vs), 792(w), 763(w), 708(vw), 558(w). HRMS-ESI: m/z, cal: 449.2440, found: 449.2451 [M]⁺. M.p. = 188-189 °C.

Acknowledgments

This work was supported by the National Natural Science Foundation of China (51372003, 21271004, 51432001, 21271003, 51472002, 21275006), Focus on returned overseas scholar of Ministry of Education of China, the Higher Education Revitalization Plan Talent Project (2013).

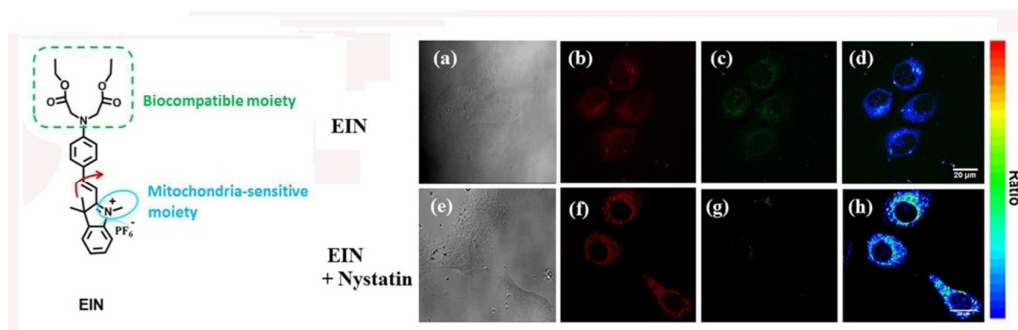
References

- M. J. Stutts, C. M. Canessa, J. C. Olsen, M. Hamrick, J. A. Cohn, B. C. Rossier and R. C. Boucher, *Science*, 1995, **269**, 847-850.
- K. Luby-Phelps, *Int. Rev. Cytol.*, 1999, **192**, 189-221.
- G. S. Zubenko, U. Kopp, T. Seto and L. L. Firestone, *Psychopharmacology (Berlin)*, 1999, **145**, 175-180.
- O. Nativ, M. Shinitzky, H. Manu, D. Hecht, C. T. Roberts, D. Leroith and Y. Zick, *Biochem. J.*, 1994, **298**, 443-450.
- G. Deliconstantinos, V. Villiotou and J. C. Stavrides, *Biochem. Pharmacol.*, 1995, **49**, 1589-1600.
- S. J. Singer and G. L. Nicolson, *Science*, 1972, **175**, 720-731.
- Z. G. Yang, J. F. Cao, Y. X. He, J. H. Yang, T. Kim, X. J. Peng and J. S. Kim, *Chem. Soc. Rev.*, 2014, **43**, 4563-4601.
- M. K. Kuimova, G. Yahioglu, J. A. Levitt and K. Suhling, *J. Am. Chem. Soc.*, 2008, **130**, 6672-6673.
- F. Liu, T. Wu, J. F. Cao, S. Cui, Z. G. Yang, X. X. Qiang, S. G. Sun, F. L. Song, J. L. Fan, J. Y. Wang and X. J. Peng, *Chem. - Eur. J.*, 2013, **19**, 1548-1553.
- Z. G. Yang, Y. X. He, J. H. Lee, N. Park, M. Suh, W. S. Chae, J. F. Cao, X. J. Peng, H. Jung, C. Kang and J. S. Kim, *J. Am. Chem. Soc.*, 2013, **135**, 9181-9185.
- A. Battisti, S. Panettieri, G. Abbandonato, E. Jacchetti, F. Cardarelli, G. Signore, F. Beltram and R. Bizzarri, *Anal. Bioanal. Chem.*, 2013, **405**, 6223-6233.
- N. Gupta, S. I. Reja, V. Bhalla, M. Gupta, G. Kaur and M. Kumar, *J. Mater. Chem. B*, 2016, **4**, 1968-1977.
- N. A. Hosny, C. Fitzgerald, A. Vysniauskas, A. Athanasiadis, T. Berkemeier, N. Uygur, U. Pöschl, M. Shiraiwa, M. Kalberer, F. D. Pope and M. K. Kuimova, *Chem. Sci.*, 2016, **7**, 1357-1367.
- S. Raut, J. Kimball, R. Fudala, H. Doan, B. Maliwal, N. Sabnis, A. Lacko, I. Gryczynski, S. V. Dzyuba and Z. Gryczynski, *Phys. Chem. Chem. Phys.*, 2014, **16**, 27037-27042.

ARTICLE

Journal Name

15. A. Vysniauskas, M. Balaz, H. L. Anderson and M. K. Kuimova, *Phys. Chem. Chem. Phys.*, 2015, **17**, 7548-7554.
16. I. Lopez-Duarte, T. T. Vu, M. A. Izquierdo, J. A. Bull and M. K. Kuimova, *Chem. Commun.*, 2014, **50**, 5282-5284.
17. F. Rashid and R. W. Horobin, *Histochem. Cell Biol.*, 1990, **94**, 303-308.
18. R. W. Horobin, J. C. Stockert and F. Rashid-Doubell, *Histochem. Cell Biol.*, 2006, **126**, 165-175.
19. R. C. Weast, CRC Handbook of Chemistry and Physics, CRC Press Inc., Boca Raton, FL, USA, 68th ed., 1987, D221-D269.
20. J. Rotzler, *Tailoring Intra-and Intermolecular Properties: From Cyclophanes to Daisy Chains*, Verlag Dr. Hut, 2012, pp. 119-126.
21. C. Ravikumar, I. H. Joe and V. Jayakumar, *Chem. Phys. Lett.*, 2008, **460**, 552-558.
22. H. C. Gerritsen and C. J. De Grauw, *Microsc. Res. Tech.*, 1999, **47**, 206-209.
23. S. M. Potter, *Curr. Biol.*, 1996, **6**, 1595-1598.
24. L. V. Chinta, L. Lindvere, A. Dorr, B. Sahota, J. G. Sled and B. Stefanovic, *NeuroImage*, 2012, **61**, 517-524.
25. Q. Zhang, X. Tian, Z. Hu, C. Brommesson, J. Wu, H. Zhou, S. Li, J. Yang, Z. Sun, Y. Tian and K. Uvdal, *J. Mater. Chem. B*, 2015, **3**, 7213-7221.
26. Y. Koide, Y. Urano, S. Kenmoku, H. Kojima and T. Nagano, *J. Am. Chem. Soc.*, 2007, **129**, 10324-10325.
27. K. H. Xu, L. L. Wang, M. M. Qiang, L. Y. Wang, P. Li and B. Tang, *Chem. Commun.*, 2011, **47**, 7386-7388.
28. D. Miguel, S. P. Morcillo, A. M. Lasanta, N. Fuentes, L. M. Fernandez, I. Corral, M. J. Ruedas-Rama, D. J. Cardenas, L. A. Cienfuegos, A. Orte and J. M. Cuerva, *Org. Lett.*, 2015, **17**, 2844-2847.
29. M. A. Haidekker, T. P. Brady, D. Lichlyter and E. A. Theodorakis, *J. Am. Chem. Soc.*, 2006, **128**, 398-399.
30. L. Wang, Y. Xiao, W. Tian and L. Deng, *J. Am. Chem. Soc.*, 2013, **135**, 2903-2906.
31. G. Thomas, J. L. Fourrey and A. Favre, *Biochemistry*, 1978, **17**, 4500-4508.
32. N. Jiang, J. Fan, S. Zhang, T. Wu, J. Wang, P. Gao, J. Qu, F. Zhou and X. Peng, *Sensor Actuat B-Chem.*, 2014, **190**, 685-693.
33. G. Zhang, Y. Sun, X. He, W. Zhang, M. Tian, R. Feng, R. Zhang, X. Li, L. Guo, X. Yu and S. Zhang, *Anal. Chem.*, 2015, **87**, 12088-12095.
34. G. Masanta, C. S. Lim, H. J. Kim, J. H. Han, H. M. Kim and B. R. Cho, *J. Am. Chem. Soc.*, 2011, **133**, 5698-5700.
35. A. R. Sarkar, C. H. Heo, H. W. Lee, K. H. Park, Y. H. Suh and H. M. Kim, *Anal. Chem.*, 2014, **86**, 5638-5641.
36. H. Zhang, R. Liu, Y. Tan, W. H. Xie, H. Lei, H. Y. Cheung and H. Sun, *ACS Appl. Mater. Interfaces*, 2015, **7**, 5438-5443.
37. G. Li, D. Zhu, L. Xue and H. Jiang, *Org. Lett.*, 2013, **15**, 5020-5023.
38. W. Liu, J. Jiang, C. Chen, X. Tang, J. Shi, P. Zhang, K. Zhang, Z. Li, W. Dou, L. Yang and W. Liu, *Inorg. Chem.*, 2014, **53**, 12590-12594.
39. A. C. Souza, F. S. Machado, M. R. Celes, G. Faria, L. B. Rocha, J. S. Silva and M. A. Rossi, *J. Vet. Med., A*, 2005, **52**, 230-237.
40. S. P. Soltoff and L. J. Mandel, *J. Membr. Biol.*, 1986, **94**, 153-161.
41. D. Li, X. Tian, A. Wang, L. Guan, J. Zheng, F. Li, S. Li, H. Zhou, J. Wu and Y. Tian, *Chem. Sci.*, 2016, **7**, 2257-2263.
42. W. Zhu, X. Huang, Z. Guo, X. Wu, H. Yu and H. Tian, *Chem. Commun.*, 2012, **48**, 1784-1786.



Convenient and rational design water-soluble two-photon excited fluorescence (TPEF) sensors for monitoring viscosity with specific targeting at subcellular level remain a challenge. Herein, we reported a novel water-soluble ratiometric TPEF chemosensor **EIN** that is specifically responsive and singularly sensitive to mitochondria viscosity in living cells. Because its fluorescence emission peaks at two different wavelengths show obvious enhancement with the increased solvent viscosity, we found that fluorescence intensity ratio (I_{569} / I_{384}) versus the logarithm of the viscosity ($\log \eta$) enable to monitor and quantify the abnormal changes of mitochondria viscosity. More importantly, **EIN** was successfully utilized to distinguish normal and nystatin treated HepG2 cells viscosity difference of mitochondria. In a word, the merits of NIR property, high selectivity and signal ratio provide more convenience for studying biological processes and mitochondria viscosity related diseases.